Clinical Biomechanics 68 (2019) 73–79

Contents lists available at ScienceDirect

Clinical Biomechanics

journal homepage: www.elsevier.com/locate/clinbiomech

Changes in intraarticular pressure on the blood supply in the retinaculum of the femoral neck

Jiong Mei[a,*,1], Fei Yan[b,c,1], Ming Ni[c], Hua Wang[d], Fangfang Zhang[d], Zhaobin Wang[d]

[a] Department of Orthopedic Surgery, Shanghai Jiao Tong University Affiliated Sixth People's Hospital, Shanghai 200233, China
[b] Laboratory of Biomechanical Engineering, Department of Applied Mechanics, Sichuan University, Room 503, Yifu Science and Technology Building, Yihuan Road, Chengdu 610065, China
[c] Interdisciplinary Division of Biomedical Engineering, The Hong Kong Polytechnic University, ST 405, No.11, Yuk Choi Road, Hung Hom, Kowloon 999077, Hong Kong, China
[d] Department of Orthopaedics, Tongji Hospital, Tongji University School of Medicine, Shanghai 200065, China

ARTICLE INFO

Keywords:
Arterial pressure
Arteries
Blood vessels
Femoral fractures

ABSTRACT

Background: This study aimed to analyze the effects of intracapsular pressure (IAP) on blood flow in the femur after a femoral neck fracture.
Methods: Four simplified vascular models were used to measure the effect of vessel length on arterial blood flow in 10 New Zealand white rabbits. Ten models were evaluated under 10 different blood pressures.
Findings: IAP increased following fracture of the femoral neck, and deformation had the greatest potential effect on blood flow in the retinacular artery. When blood pressure was fixed at 60 mm Hg, an increase in IAP caused a reduction in blood flow. When the IAP was relatively high (above 60 mm Hg), and higher than the blood pressure, blood flow continued to drop as intracapsular pressure increased. Shortening of blood vessels had no significant effect on blood supply. However, the *p*-value was uniformly significant (< 0.05) when stretched and twisted blood vessels were compared with normal blood vessels.
Interpretation: The results of computational fluid-structure interaction similarly indicated that a smaller blood vessel diameter and twisted blood vessels will result in decreased flow velocity when IAP increases. This study also revealed a close relationship between IAP and the hip joint's position and traction.

1. Introduction

Currently, there is no reliable way to assess the degree of impairment to the femoral head blood supply caused by a femoral neck fracture. When such a fracture occurs within the capsule of the femoral neck, bleeding from the fracture end increases pressure within the sealed capsule, compressing the blood vessels of the retinaculum on the surface of the femoral neck, and ultimately interfering with the blood supply to the femoral head (Soto-Hall et al., 1964; Zlotorowicz et al., 2011). At the same time, displacement of the fracture end from impaction, separation and rotation may also cause compression, stretching, twisting or even breakage of the blood vessels of the retinaculum, which will worsen blood flow to the femoral head (K., 1997; Kalhor et al., 2009).

More than 50 years after Soto-Hall and associates first proposed the concept of intra-articular pressure (IAP) increase after fracture of the femoral neck (Soto-Hall et al., 1964), and after years of observational research, the effect of IA pressure on the blood supply to the femoral head and on the development of necrosis of the femoral head after fracture of the femoral neck is still a matter of dispute (Crawfurd et al., 1988).

With advances in vascular imaging technology and anatomical knowledge, it has become known that blood reaching the femoral head is chiefly supplied by the retinacular artery in the circumflex femoral arterial ring (Kalhor et al., 2009; Zlotorowicz et al., 2011). This artery enters through the capsule at the attached portion of the femoral neck, and passes through the deep portion of the synovial plica of the femoral neck. Beneath the synovial membrane, a branch of the artery enters the nutrient foramen on the femoral neck, or enters the femoral head. As a result, the length of the intracapsular retinacular artery is relatively fixed (K., 1997; Kalhor et al., 2009).

The geometries of the vessels in the femoral head change after

* Corresponding author at: Department of Orthopedic Surgery, Shanghai Jiao Tong University Affiliated Sixth People's Hospital, 600 Rd. Yishan, Shanghai 200233, China.
E-mail address: meijiong@sjtu.edu.cn (J. Mei).
[1] These authors contributed equally.

https://doi.org/10.1016/j.clinbiomech.2019.05.026
Received 12 July 2017; Accepted 15 May 2019

femoral neck fracture; the vessels become elongated and curved (Holmberg and Dalen, 1987; Smith, 1959; Swiontkowski et al., 1990). The changes in vascular geometries have an influence on the blood flow. Moreover, the changes in blood flow play a significant role in the development of osteonecrosis (Garden, 1971; Holmberg and Dalen, 1987; Strömqvist, 1983; Strömqvist et al., 1988). Thus, we aimed to investigate how the changes in vascular geometries affect blood flow through using computational simulation. We developed an in vitro experimental study using laboratory animals to observe the effects of increased intracapsular pressure on blood flow in the femur. Computational fluid-structure interaction was performed to study and verify the effect of pressure changes around blood vessels on blood flow within the vessels.

2. Methods

2.1. In vitro vascular experiment

2.1.1. Source of blood vessel specimens

The first step was to establish a standard measurement for the diameters of blood vessels in the human retinaculum, according to numerous reports in the literature. For the superior retinacular artery, the external diameter where the artery passes through the capsule is 1.0–1.6 mm, and the maximum length from the point where the artery enters the capsule to the femoral head is 1.6–2.6 cm. Next, for the inferior retinacular artery, the external diameter where the artery passes through the capsule is 0.4–1.4 mm, and the intracapsular length is 1.5–2.4 cm. Third, the external diameter where the anterior retinacular artery passes through the capsule is 0.4–1.0 mm, and the intracapsular length is 1.6–2.1 cm.

To mimic the average diameter of the human retinacular artery, we used a section of abdominal aorta taken from healthy New Zealand male white rabbits. The rabbits weighed from 2.0 to 2.5 kg, and had blood vessel diameters ranging from 1.8 to 2.0 mm. We used a 4-cm segment of rabbit aorta to mimic the human retinacular artery in the in vitro experiment.

2.1.2. Design of the experimental apparatus

All protocols and procedures were approved by our Institutional Animal Care and Use Committee. These rabbits were maintained in an animal facility under specific pathogen-free conditions and treated in accordance with the institutional guidelines for animal care during research. This experiment used abdominal aortas from 10 4-to-6-week-old male laboratory rabbits to simulate the retinacular artery of the femoral neck in humans. A 4-cm length of aorta, approximately 2 mm in diameter, was removed from each of the 10 rabbits.

2.2. Experimental instruments and apparatus

The experimental instruments and apparatus are shown in Fig. 1. A multichannel biosignal collection and processing system (model RM6240SD, produced by the Chengdu Instrument Co, Chengdu, PRC) was provided by the Physiology Teaching Research Laboratory of Shanghai Tongji University. After connection to a computer, RM6240SD biosignal collection and processing system 2.0z software was used to measure intravascular pressure and extravascular intracapsular pressure inside a 2-cm T-shaped three-way glass tube in real-time.

The three-way glass tube had three openings, or mouths. The glass tube was 10 cm long, 5 cm in height, and 2 cm in diameter, and all three mouths could be sealed with rubber stoppers. The disposable intravenous infusion tubing (0.55*20 II RW LB, Zhejiang KDL Medical Equipment Stock Co, Ltd.; Wenzhou, China) (Fig. 1, A and B), which had a diameter of approximately 1.5 mm, was inserted through holes bored in the rubber stoppers, and the stoppers were then sealed with hot glue (Hot Glue Sticks, Ziyou Shandong Yongjiu Jiaonian Zhipin Co Ltd.). Standard measuring cylinders (100 mL, 50 mL, and 10 mL), and a standard steel frame and test tube clamps (all from Taizhou Yuxiu Trading Co, Ltd.) were also used. A medical three-way valve (Shanghai Beite Medical Appliance Co, Ltd., Shanghai, China) completed the apparatus.

2.3. Insertion of the blood vessel

The blood vessel was placed in the three-way glass tube. Rubber stoppers were used to seal the two mouths and upper mouth of the glass tube, which simulated the human hip capsule. The two ends of the blood vessel were inserted into the disposable intravenous infusion tubing and then were tied with thread.

The disposable intravenous infusion tubing (and blood vessel) was passed horizontally through the glass tube, and connected with the rubber stoppers and external equipment on both ends. Disposable intravenous infusion tubing was passed through the right rubber stopper, so that it was at the same height as the blood vessel. The left end of the blood vessel was connected with one mouth (Fig. 1, D) of the medical three-way valve. Mouth E (Fig. 1) of the three-way valve was connected with channel 4 (used to measure intravascular pressure) of the multichannel biosignal collection and processing system. As seen in Fig. 1, mouth F of the three-way valve was connected with a 500-mL physiological saline infusion bottle (Shandong Pharmaceutical Glass Co, Ltd., Shandong, China). To simulate blood pressure, the infusion bottle was hung at a height of 81 cm, creating 60 mm Hg of pressure. The right end of the blood vessel was connected with a standard measuring cylinder using hose B (Fig. 1). Three measurements were taken during 10-minute intervals, and the 1-minute flow volume indicator calculated the flow volume. As shown in Fig. 1, hose C was connected with channel 1 of the multichannel biosignal collection and processing system. Mouth G of the T-shaped three-way glass tube was connected with 500-mL infusion bottle b (used to simulate intracapsular pressure). The bottle was mounted at a height of approximately 0 cm to 108 cm, which generated 0–80 mm Hg of pressure.

2.3.1. Geometric models

Four simplified vascular models were established in order to investigate the effect of vessel length on blood flow in the arteries. Specifically, the original model (Original) was a straight 40-mm-long tube. The second model (Elongated) used a 50-mm-long straight tube. The third model (C-type) was a circular arc tube with a 40-mm arc length and a straight-line distance from inlet to outlet of 35 mm (Fig. 2a). The last model (S-type) used an S-type tube, 40 mm long, with a 35-mm straight-line distance from inlet to outlet (Fig. 2b). Moreover, the diameter and wall thickness of these vessels at the inlet and outlet were 1.0 mm and 0.12 mm, respectively.

The four geometric models were meshed with hexahedral elements in ANSYS 14.0 software (ANSYS, Inc., Canonsburg, PA, USA). The serial numbers of the four elements are 79098, 89135, 105842, and 111404, respectively.

2.3.2. Computational fluid-structure interactions

To investigate how the external pressure applied to the arterial wall affects blood flow in the vessel, the computational fluid-structure interaction (FSI) of blood and arterial wall was conducted with ANSYS 14.0 based on the arbitrary Lagrangian-Eulerian (ALE) method. A structural analysis and a corresponding computational fluid dynamic (CFD) analysis were conducted in this FSI simulation. The fluid pressure at the boundary was used as the load on the structural analysis, while the resulting displacement, velocity, and acceleration acquired in the structural analysis were passed on as the boundary conditions of the CFD analysis. These analyses under the interaction continued until the equilibrium of the solutions between the structural analysis and the CFD analysis was reached. More specifically, the meshed model of vascular wall was imported into the “Transient structural” module of

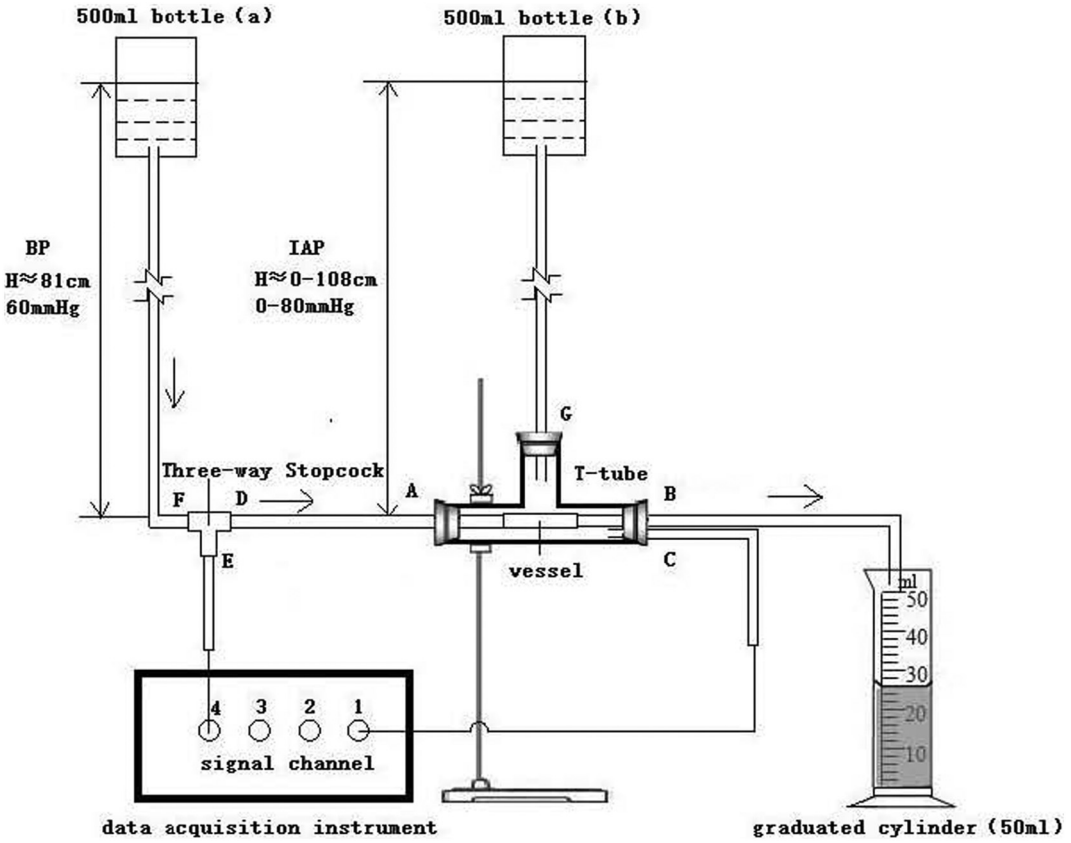

Fig. 1. An illustration demonstrating the experimental equipment and apparatus used in our study. Note the 3-way glass tube with 3 openings, or mouths (A, B, G) and the 3-way valve or stopcock (D, E, F). To simulate blood pressure (BP), a 500-mL infusion bottle (a) was hung at a height of 81 cm, to create 60 mm Hg of pressure. A second 500-mL bottle (b) was mounted at approximately 0 cm to 108 cm to generate 0–80 mm Hg of simulated intra-arterial pressure (IAP). A graduated cylinder (50 mL) received the flow.

ANSYS software for the simulation of the arterial wall, while the meshed model of blood vessel was imported into ANSYS Fluent software for the simulation of blood flow. In addition, the coupled simulation of blood and arterial wall was carried out in the ANSYS module "System Coupling." In this coupling, the blood flow and arterial wall motion were calculated iteratively within each time point under the external pressure applied on the wall surface. The total time of the simulation was 7 s.

2.3.3. Governing equations

In our computational simulation, the blood was assumed to be homogeneous, incompressible fluid (Smith, 1959). In terms of blood flow in the FSI, the three-dimensional Navier-Stokes equation and continuity equation were employed with treatment of moving domain. These equations describe how the velocity, pressure, temperature, and density of a moving fluid are related. The continuity equation (Eq. (1)) is:

$$\frac{d}{dt}\int_{V(t)}\rho dV + \int_s \rho(u_j - w_j)dn_j = 0 \tag{1}$$

The Navier-Stokes equation (Eq. (2)) is as follows:

$$\frac{d}{dt}\int_{V(t)}\rho u_i dV + \int_s \rho(u_j - w_j)u_i dn_j = -\int_s P dn_j + \int_s \mu\left(\frac{\partial u_i}{\partial x_j} + \frac{\partial u_j}{\partial x_i}\right)dn_j \tag{2}$$

In these equations, u_j and w_j are the blood velocity and the velocity of the control volume boundary, respectively, and P is the pressure. V and s represent the integrated volume and surface, respectively, and dn_j is the differential Cartesian components of the outward normal surface

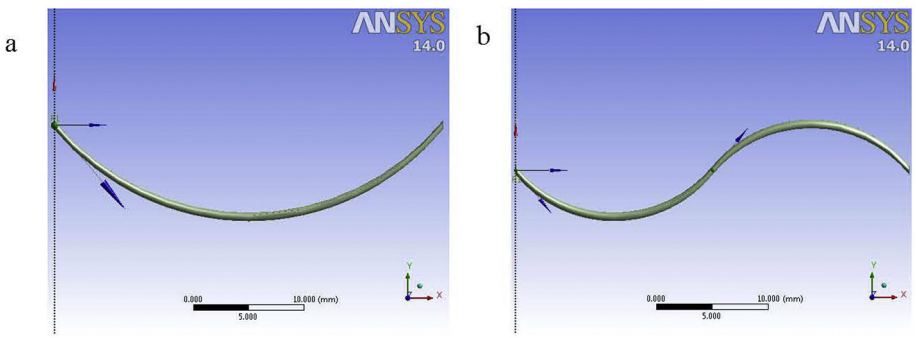

Fig. 2. Geometries of the C-type vessel (a) and the S-type vessel (b).

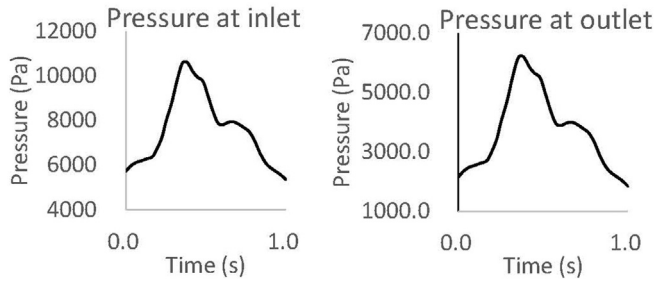

Fig. 3. Two figures demonstrate the pressure (pa) measured over 1 s at the inlet (left) and outlet (right).

vector. Moreover, ρ and μ are the density and dynamic viscosity of blood, respectively: $\rho = 1050\,kg/m^3$, $\mu = 3.5 \times 10^{-3}\,kg/ms$ (Olufsen et al., 2000).

In terms of transient structural simulation, momentum balance equations were solved with fluid-solid interface boundary and constraint conditions. Additionally, the density and Poisson's ratio of the arterial wall were $1060\,kg/m^3$ and 0.49 (Kim et al., 2009), respectively. Young's modulus of the vascular wall was set as 3.06 MPa (Wentzel et al., 2001).

In the transient structural simulation, 80 mm Hg external pressure was applied on the outside surface of the vascular wall. The fluid-solid interface was employed on the interface between the blood and tissue. At the interface, the blood pressure acquired in the CFD analysis was transferred to the structural model as a load. Moreover, two ends of the vascular wall were fixed.

2.3.4. Boundary conditions

In the blood flow simulation, the boundary conditions of pressure-inlet and pressure-outlet were applied in the inlet and outlet of the blood vessel, respectively. The pressure curves (Fig. 3) were based on reports in the literature (Holmberg and Dalen, 1987; Wentzel et al., 2001). Moreover, smoothing and remeshing were applied in dynamic mesh setting. The mesh was moved according to the data obtained by the structural analysis.

2.4. Statistical analysis

Data were summarized as mean with the standard error of the mean (SEM) for given pressures and vessel types. A repeated-measures factorial ANOVA was applied for identifying the effects upon blood volume, mL/per minute, from the pressures or the types. A pair-wise comparison, Bonferroni test, was applied to compare the difference between two pressures or between two types. All statistical assessments were two-tailed and considered significant as $p < 0.05$. All statistical analyses were carried out with IBM SPSS statistical software version 22 for Windows (IBM Corp, Armonk, NY).

3. Results

3.1. Experimental content

Stretching and twisting of blood vessels affects their blood supply. When a fracture of the femoral neck occurs, displacement of the fracture end, including shortening, separation, and rotation, may also cause compression, stretching, and twisting. Thus, the retinacular artery may be shortened, stretched, or twisted. Apart from direct damage to blood vessels caused by the fracture, the deformation of blood vessels by the fracture may also affect the blood supply. When the blood pressure was a constant 60 mm Hg (as described previously in this article), blood pressure in the lateral and medial femoral circumflex artery was approximately 40–80 mm Hg.

This experiment was a fully quantitative assessment of the blood supply to the femoral head and neck. As a consequence, in comparison with qualitative or semi-quantitative assessment procedures, we believe the results of this experiment had a higher level of accuracy.

Table 1
Blood volume (mL/per min) with four vessel types tested under 10 different pressures.

Pressure (mm Hg)	Vessel types				p-Value[2]	p-Value[3]	p-Value[4]
	Type A	Type B	Type C	Type D			
0	45.36	45.3	40.94	35.29	1.000	< **0.001**	< **0.001**
10	44.35	44.63	40.17	34.22	0.532	< **0.001**	< **0.001**
15	43.85	43.76	39.51	33.24	1.000	< **0.001**	< **0.001**
20	42.71	42.87	38.24	32.55	1.000	< **0.001**	< **0.001**
25	42.12	42.08	37.42	31.56	1.000	< **0.001**	**0.001**
30	41.37	41.2	36.67	30.77	0.697	< **0.001**	< **0.001**
35	40.65	40.47	36	29.93	1.000	< **0.001**	< **0.001**
40	39.88	39.72	35.39	29.31	0.797	< **0.001**	< **0.001**
60	38.9	38.89	34.17	28.18	1.000	< **0.001**	< **0.001**
80	37.76	37.82	32.99	27.15	1.000	< **0.001**	< **0.001**

Blood volume was summarized as mean for each of vessel types under different pressures ($n = 10$).
[2–4]Comparisons between A vs. B[2], A vs. C[3], and A vs. D.[4]
p-Values in bold type indicate significant results ($p < 0.05$).

Table 1 summarizes the dispersion of blood volume per minute for specific vessel types and pressures. The blood volume ranged from 45.36 to 37.76 mL, from 45.3 to 37.8 mL, from 40.9 to 32.9 mL, and 35.3 to 27.1 mL for vessel types A, B, C, and D, respectively. For each vessel type, the mean blood volume was decreased along with the increasing pressure (Table 2).

Furthermore, the blood volume for both vessel types C and D was represented as lower than for vessel type A under the 10 different pressures (all $p < 0.05$). There was no significant difference shown between vessel types A and B (Table 1).

As shown in Fig. 4, the change in the distance from inlet to outlet within a vessel influenced blood flow. The increment and reduction of the distance from inlet to outlet contributed to the increase in vascular resistance of the Elongated, C-type, and S-type models. Thus, mass flow rates of Elongated, C-type and S-type models were smaller than those of the Original type model. Moreover, the mass flow rate of the Elongated model was greater than the mass flow rates of the C-type and S-type models, possibly due to the change in the geometry of C-type and S-type models. In summary, the changes in vascular geometries contributed to the reduction of blood flow, and the bending deformation caused a larger decrease in blood flow compared to elongation. Consequently, the change in the geometry of a vessel could cause a greater increase in vascular resistance compared with simple elongation.

4. Discussion

In current clinical practice, there are two major approaches to assessing the blood supply to the femoral head and neck: qualitative and semi-quantitative judgment. The former approach includes measuring blood flow, and ordering enhanced magnetic resonance imaging and routine radionuclide planar imaging. The latter type of imaging includes laser Doppler flowmetry (LDF), single-photon emission computed tomography (SPECT), positron emission tomography (PET), and positron emission tomography and computed tomography (PET-CT), for example (L., 2008; Lang et al., 1993; Radegran, 1997). Regardless of the method used, it is difficult to accurately assess the degree of femoral head ischemia, which means that the clinical application of these methods remains somewhat restricted (Alberts, 1990; Asnis et al., 1994; Dasa et al., 2008; Seo et al., 2008; Sugamoto et al., 1998; Yang et al., 2004).

Because the intracapsular length of the human retinacular artery is approximately 1.5–2.6 cm long, in order to simulate the length using an

Table 2
Significance* of pair-wise comparison between pressures for each vessel type.

Vessel type	Pressure	Pressure (mm Hg)									
		0	10	15	20	25	30	35	40	60	80
A	10	**0.059**	–								
	15	**0.002**	0.536	–							
	20	**< 0.001**	**< 0.001**	**0.012**	–						
	25	**< 0.001**	**< 0.001**	**< 0.001**	**0.002**	–					
	30	**< 0.001**	**< 0.001**	**< 0.001**	**< 0.001**	**< 0.001**	–				
	35	**< 0.001**	**< 0.001**	**< 0.001**	**0.001**	**0.006**	0.191	–			
	40	**< 0.001**	**< 0.001**	**< 0.001**	**0.001**	**0.004**	**0.041**	0.064	–		
	60	**< 0.001**	**< 0.001**	**< 0.001**	**< 0.001**	**0.001**	**0.004**	**0.011**	0.064	–	
	80	**< 0.001**	**< 0.001**	**< 0.001**	**0.001**	**0.002**	**0.006**	**0.006**	**0.010**	0.064	–
B	10	**0.034**	–								
	15	**0.012**	0.118	–							
	20	**0.004**	**0.008**	**0.047**	–						
	25	**< 0.001**	**< 0.001**	**< 0.001**	**0.025**	–					
	30	**< 0.001**	**< 0.001**	**< 0.001**	**< 0.001**	**0.001**	–				
	35	**< 0.001**	**< 0.001**	**< 0.001**	**< 0.001**	**0.009**	0.348	–			
	40	**< 0.001**	**< 0.001**	**< 0.001**	**< 0.001**	**0.002**	**0.017**	0.351	–		
	60	**< 0.001**	**< 0.001**	**< 0.001**	**< 0.001**	**0.001**	**0.004**	**0.034**	0.097	–	
	80	**< 0.001**	**< 0.001**	**< 0.001**	**< 0.001**	**0.001**	**0.002**	**0.008**	**0.007**	**0.010**	–
C	10	**0.001**	–								
	15	**0.001**	**0.003**	–							
	20	**< 0.001**	**< 0.001**	**< 0.001**	–						
	25	**< 0.001**	**< 0.001**	**< 0.001**	**0.006**	–					
	30	**< 0.001**	**< 0.001**	**< 0.001**	**0.002**	0.076	–				
	35	**< 0.001**	**< 0.001**	**< 0.001**	**< 0.001**	**0.001**	**0.020**	–			
	40	**< 0.001**	**< 0.001**	**< 0.001**	**< 0.001**	**< 0.001**	**0.003**	0.152	–		
	60	**< 0.001**	**< 0.001**	**< 0.001**	**< 0.001**	**< 0.001**	**0.001**	**0.005**	**0.002**	–	
	80	**< 0.001**	**< 0.001**	**< 0.001**	**0.001**	**0.001**	**0.004**	**0.017**	**0.019**	0.261	
D	10	**0.013**	–								
	15	**0.001**	**0.001**	–							
	20	**0.001**	**0.005**	0.544	–						
	25	**< 0.001**	**< 0.001**	**0.001**	**0.008**	–					
	30	**< 0.001**	**< 0.001**	**< 0.001**	**< 0.001**	**0.008**	–				
	35	**< 0.001**	**0.001**	**0.003**	**0.001**	**0.021**	0.529	–			
	40	**< 0.001**	**< 0.001**	**0.001**	**< 0.001**	**0.002**	**0.015**	0.058	–		
	60	**< 0.001**	**< 0.001**	**< 0.001**	**< 0.001**	**0.001**	**0.005**	**0.015**	**0.047**	–	
	80	**< 0.001**	**< 0.001**	**< 0.001**	**< 0.001**	**< 0.001**	**0.001**	**0.003**	**0.004**	**0.004**	–

p-Values in bold type indicate significance ($p < 0.05$).
* Results were represented as *p*-values.

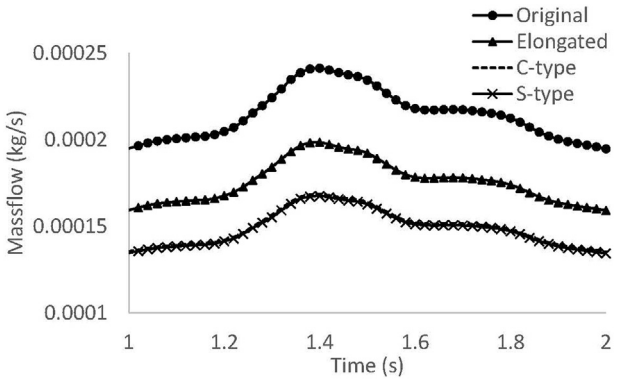

Fig. 4. The outlet mass flow (kg/s) of the four computational models.

animal model, disposable intravenous infusion tubing had to be inserted into the two ends of the blood vessel, and a thread was then used to fasten the tubing and blood vessel. As a result, the section of blood vessel used was longer than the actual intracapsular length in humans. And, while the human retinacular artery has a diameter of approximately 0.4–1.6 mm, the outer diameter of the rabbit blood vessel used in this experiment was approximately 2.0–2.5 mm. (The rabbits weighed approximately 2.0–2.5 kg, so the diameter of the rabbits' abdominal aortas was calculated as 0.8079 × body weight [kg] + 0.3795) (Wang and T., 1985).

Because rabbit abdominal aortas are easy to remove, readily available, and have a diameter similar to that of the human retinacular artery, we chose to use rabbit abdominal aortas instead of human retinacular arteries. And, because the human retinacular artery is located within the retinaculum, lies close to the surface of the femoral neck, and is relatively immobile, this experiment placed the blood vessels in a suspended situation, with evenly distributed applied forces in all directions, in order to simulate human blood vessel shortening, stretching, and twisting (Mei et al., 2015).

From our analysis of the relationship between the femoral neck, retinaculum, and retinacular artery, we observed that when the retinaculum undergoes displacement due to fracture of the femoral neck, the blood vessels located in the retinaculum have a protective effect. Based on this consideration, the blood vessel twisting in this study's computational fluid-structure interaction was similar to the twisting displacement of the retinacular artery that would occur after an actual fracture of the femoral neck, and reflected the anatomical characteristics of the retinacular artery.

4.1. Analysis of the effect of different blood vessel morphologies on blood supply

After a fracture of the femoral neck, the fracture end may undergo shortening, separation, or even twisting displacement. The retinacular artery, which runs along the bone of the femoral neck will also undergo displacement. As a result, when a fracture occurs, the retinacular artery inevitably undergoes a certain degree of shortening, stretching, or even

twisting.

This experiment varied the intracapsular and blood vessel morphology at a blood pressure of 60 mm Hg, and relied on the measurement of 1-minute fluid discharge to quantitatively demonstrate that an increase in intracapsular pressure will cause lower blood vessel discharge, as will blood vessel stretching and twisting. Stretching caused an average decrease of 11.3%, while twisting caused an average of decrease of 25.6%, which was sufficient to influence the blood supply. In contrast, blood vessel shortening had no significant effect on blood vessel discharge.

t-Test analysis of the results of pairwise experiments involving the comparison of blood vessels that had undergone shortening, stretching, and twisting with blood vessels in their normal state indicated that the *p*-value was uniformly > 0.05 when shortened blood vessels were compared with the original blood vessels (10 blood vessel specimens). This indicates that the shortening of blood vessels has no significant effect on blood supply. However, the *p*-value was uniformly < 0.05 when stretched and twisted blood vessels were compared with normal blood vessels.

We concluded that the stretching and twisting of blood vessels will affect their blood supply. The results of computational fluid-structure interaction similarly indicate that a smaller blood vessel diameter (such as a diameter of 0.5 mm) and twisted blood vessel (such as a diameter of 1 mm and 90° twisting) will result in decreased flow velocity when intracapsular pressure increases. For instance, under the same intracapsular pressure, a blood vessel with a smaller diameter and twisting will have significantly lower flow velocity than a blood vessel with a diameter of 1 mm. (In this study, flow velocity decreased by an average of 69.5% when the vessel diameter was smaller, and also decreased by an average of 71.5% when the blood vessel had undergone twisting.)

These results suggest that when reduction and internal fixation are performed on fractures of the femoral neck, anatomical reduction is more important than pressure reduction by means of intracapsular suction during emergency treatment or postsurgical opening of the capsule.

4.2. Effect of increased intracapsular pressure on blood supply

As for the mechanism involved in ischemic necrosis of the femoral head following fracture of the femoral neck, the universally accepted view is that trauma causes direct injury to the blood vessels supplying the femoral head and neck, especially the superior retinacular artery. However, results of some digital subtraction analyses (DSAs) and emission computer tomography (ECT) studies have shown that some patients without evident impairment of the blood supply to the femoral head and neck still develop necrosis of the femoral head after their injury, regardless of whether internal fixation has been performed (Dasa et al., 2008; Mei et al., 2017; Soto-Hall et al., 1964). The explanation for this phenomena is still greatly in dispute. In particular, an increase in intravascular pressure (IAP) following fracture of the femoral neck has been suggested as a cause for the impaired blood supply; this has been experimentally verified, and the effect of IAP is receiving growing attention from clinical physicians and researchers.

Bonnaire et al. and other researchers (Beck et al., 2004; Bonnaire et al., 1998; Drake and Meyers, 1984; Holmberg and Dalen, 1987) employed experiments to verify that an increase in IAP will reduce circulation to the femoral head and neck, which will then significantly influence the critical value of the blood supply. According to these authors, intracapsular pressure must be > 40 mm Hg. Beck and colleagues (Beck et al., 2004) believe that the intracapsular pressure must be > 58 mm Hg, while Drake and Meyers (Drake and Meyers, 1984) and Holmberg and Dalen (Holmberg and Dalen, 1987) suggest that intracapsular pressure must be > 80 mm Hg before the blood supply to the femoral head will be affected. In addition, Drake and Meyers also measured the intracapsular pressure and degree of hematoma in patients with fracture of the femoral neck, and found an average intracapsular pressure of 29 mm Hg (range: 0–68 mm Hg) (Drake and Meyers, 1984). When Soto-Hall et al. (1964) performed similar measurements, they reported an average intracapsular pressure of 18 mm Hg. While the researchers initially believed that such minor hematomas and an intracapsular pressure less than diastolic pressure would almost certainly not affect the blood supply to the femoral head, our experimental study results involving 10 blood vessel specimens indicated that when blood pressure is stable at 60 mm Hg, as intracapsular pressure gradually increases (from 0 to 80 mm Hg), the blood discharge from blood vessels with different morphologies uniformly display a decreasing trend. Furthermore, the results of computational fluid-structure interaction examining three types of arteries undergoing five blood pressure cycles revealed that blood flow velocity tends to display a decreasing trend when the intracapsular pressure is gradually increased (0, 20, and 40 mm Hg). As a consequence, even a relatively low intracapsular pressure, such as 29 mm Hg or 18 mm Hg, will affect the blood supply to the femoral head and neck. Thus, there is no single critical value.

This study also revealed a close relationship between IAP and the hip joint's position and traction. Wu Kai et al. (Wu, 2000) sought to determine experimentally the effect of hip joint position and traction on IAP, and found that internal twisting induced the greatest increase in IAP, resulting in IAP values in the range of 37–78 mm Hg, with a maximum value of only 78 mm Hg. After examining various changes in the hip joint position, Strömqvist et al. (1988) found that the maximum IAP value (280 mm Hg to 300 mm Hg) occurred when the hip joint was extended and underwent internal twisting. This is far higher than the venous pressure at the femoral head (10–20 mm Hg). Since the pressure ordinarily does not exceed 30 mm Hg, and is even higher than normal human diastolic or systolic pressure, it would be impossible for even an intact retinacular artery or extracapsular artery to overcome this resistance when entering the capsule. Wu Kai et al. found a maximum value of only 78 mm Hg in his group's experiment (Wu, 2000). In this study, when the vascular pressure was 60 mm Hg, although blood flow was reduced somewhat when the intracapsular pressure rose to 80 mm Hg, blood still flowed into the capsule, and the blood vessel was not totally constricted. This occurred not because the intracapsular pressure was higher than the blood pressure, but merely that circulation was restricted. Because clinical experience indicates that IAP will not rise excessively after fracture of the femoral neck (Drake's research found an increase in intracapsular pressure of 0 to 68 mm Hg, while Soto-Hall found an average intracapsular pressure increase of only 18 mm Hg), the increase of 280–300 mm Hg measured by Strömqvist and colleagues following the application of a special posture and traction actually has no great clinical significance.

4.3. Effective clinical measures to reduce intracapsular pressure on blood supply

Crawfurd et al. (1988) and Holmberg and Dalen (1987) suggest that early puncture of the hip capsule to reduce pressure following fracture of the femoral neck may help reduce necrosis and collapse of the femoral head. Bonnaire et al. (Bonnaire et al., 1998; Kalhor et al., 2009) suggest that suction is an effective method of reducing joint pressure, and may even facilitate reducing capsule pressure to 0. Beck et al. and Chinese researchers (Beck et al., 2004; Wu, 2000) also believe that hematoma suction to reduce joint pressure can restore circulation to the femoral head.

Our results indicate that IAP will increase following fracture of the femoral neck, and deformation will have the greatest potential effect on blood flow in the retinacular artery. This suggests that rapid anatomical reduction following a fracture is even more important than pressure-reduction measures.

It has been reported in the literature (Liu et al., 2002) that veins in the femoral head from 15 to 20 branches on the surface of the femoral

head. These veins then form a radiating pattern centered on the highest point on the femoral head. They flow toward the boundary of the head and neck, drain out from the bone at the boundary of the head and neck, and converge into the corresponding retinaculum vein. (The veins flowing through the bone in the concave portion of the femoral head continue toward the femoral head ligament, and ultimately converge into the femoral head ligament vein.) However, there is no detailed literature concerning the anatomical morphology of the femoral retinaculum vein, making it difficult to perform analog experiments.

The results of our experiment showed the following:

(1) When blood pressure was fixed at 60 mm Hg, a rise in intracapsular pressure caused a reduction in blood flow. When the intracapsular pressure was relatively high (above 60 mm Hg), and higher than the blood pressure, blood flow continued to drop as intracapsular pressure increased. However, an increase in intracapsular pressure did not compress the blood vessel to the point that circulation was blocked completely. (2) When blood pressure was fixed at 60 mm Hg, if shortening of the blood vessel occurred, changes in blood flow with increasing intracapsular pressure were generally similar to those of the original blood vessel. When stretching and twisting occurred, blood flow decreased compared with flow in the original blood vessel (stretching caused an average decrease of 11.3%, while twisting caused an average of decrease of 25.6%), and twisting caused the most significant decrease in blood flow. (3) When intracapsular pressure gradually rose because the blood vessel was compressed, the degree of morphologic deformation gradually decreased, and blood flow velocity also gradually fell. When the blood vessel diameter was small (for example, 0.5 mm) or had morphological twisting (such as blood vessel diameter of 1 mm and 90° of twisting), the flow velocity dropped significantly compared with a blood vessel with a diameter of 1 mm. In the latter case, flow velocity decreased by an average of 69.5% when the blood diameter was smaller, and also decreased by an average of 71.5% when the blood vessel had undergone twisting. Twisting caused the most significant decrease in blood flow.

4.4. Limitations of the study

This study only considered the effect of intracapsular pressure on blood supply from the retinacular artery, and did not examine the effect of an increase in intracapsular pressure on the venous flow in the retinaculum.

Declaration of Competing Interest

None declared.

Funding

This study was supported by the National Natural Science Foundation of China [grant number: 81271991].

Ethical approval

All protocols and procedures were approved by our Institutional Animal Care and Use Committee.

Author contributions

Jiong Mei and Fei Yan designed the experiments. Hua Wang, Ming Ni, Zhaobin Wang and Fangfang Zhang performed the experiments and collected the data. Ming Ni and Fei Yan analyzed the data. Ming Ni, Fei Yan, Hua Wang and Fangfang Zhang prepared the figures and the manuscript, and Jiong Mei revised the manuscript.

References

Alberts, K.A., 1990. Prognostic accuracy of preoperative and postoperative scintimetry after femoral neck fracture. Clin. Orthop. Relat. Res. (250), 221–225.
Asnis, S.E., Gould, E.S., Bansal, M., Rizzo, P.F., Bullough, P.G., 1994. Magnetic resonance imaging of the hip after displaced femoral neck fractures. Clin. Orthop. Relat. Res. (298), 191–198.
Beck, M., Siebenrock, K.A., Affolter, B., Nötzli, H., Parvizi, J., Ganz, R., 2004. Increased intraarticular pressure reduces blood flow to the femoral head. Clin. Orthop. Relat. Res. 424, 149–152.
Bonnaire, F., Schaefer, D.J., Kuner, E.H., 1998. Hemarthrosis and hip joint pressure in femoral neck fractures. Clin. Orthop. Relat. Res. 353, 148–155.
Crawfurd, E.J., Emery, R.J., Hansell, D.M., Phelan, M., Andrews, B.G., 1988. Capsular distension and intracapsular pressure in subcapital fractures of the femur. J. Bone Joint Surg. (Br.) 70, 1958.
Dasa, V., Adbel-Nabi, H., Anders, M.J., Mihalko, W.M., 2008. F-18 fluoride positron emission tomography of the hip for osteonecrosis. Clin. Orthop. Relat. Res. 466, 1081–1086.
Drake, J.K., Meyers, M.H., 1984. Intracapsular pressure and hemarthrosis following femoral neck fracture. Clin. Orthop. Relat. Res. (182), 172–176.
Garden, R., 1971. Malreduction and avascular necrosis in subcapital fractures of the femur. J. Bone Joint Surg. 53, 183–197.
Holmberg, S., Dalen, N., 1987. Intracapsular pressure and caput circulation in non-displaced femoral neck fractures. Clin. Orthop. Relat. Res. (219), 124–126.
K., D.N., 1997. Blood flow in arteries. Annu. Rev. Fluid Mech. 29, 399–434.
Kalhor, M., Beck, M., Huff, T.W., Ganz, R., 2009. Capsular and pericapsular contributions to acetabular and femoral head perfusion. J. Bone Joint Surg. Am. 91, 409–418.
Kim, Y., Lim, S., Raman, S., Simonetti, O., Friedman, A., 2009. Blood flow in a compliant vessel by the immersed boundary method. Ann. Biomed. Eng. 37, 927–942.
L., Z.R., 2008. The early detection and reasonable treatment of femoral head necrosis. Chin. J. Joint Surg. (Electron. Edit.) 2, 1–3.
Lang, P., Mauz, M., Schörner, W., et al., 1993. Acute fracture of the femoral neck: assessment of femoral head perfusion with gadopentetate dimeglumine-enhanced MR imaging. AJR Am. J. Roentgenol. 160, 335–341.
Liu, Y., Junqing, H.U., Zhong, Z.Y., 2002. Anatomy of the intra- and extra-osteal venous drainage in femoral head and neck. Chin. J. Clin. Anat. 20, 4314.
Mei, J., Ni, M., Wang, G., et al., 2015. Association between injury to the retinacula of Weitbrecht and femoral neck fractures: anatomical and clinical observations. Int. J. Clin. Exp. Med. 8, 17674–17683.
Mei, J., Ni, M., Wang, G., et al., 2017. Number and distribution of nutrient foramina within the femoral neck and their relationship to the retinacula of Weitbrecht: an anatomical study. Anat. Sci. Int. 92, 91–97.
Olufsen, M.S., Peskin, C.S., Kim, W.Y., Pedersen, E.M., Nadim, A., Larsen, J., 2000. Numerical simulation and experimental validation of blood flow in arteries with structured-tree outflow conditions. Ann. Biomed. Eng. 28, 1281–1299.
Radegran, G., 1997. Ultrasound Doppler estimates of femoral artery blood flow during dynamic knee extensor exercise in humans. J. Appl. Physiol. 83, 1383–1388.
Seo, Y., Mari, C., Hasegawa, B.H., 2008. Technological development and advances in single-photon emission computed tomography/computed tomography. Semin. Nucl. Med. 38, 177–198.
Smith, F., 1959. Effects of rotatory and valgus malpositions on blood supply to the femoral head. J. Bone Joint Surg. Am. 41, 800–815.
Soto-Hall, R., Johnson, L.H., Johnson, R.A., 1964. Variations in the Intra-articular pressure of the hip joint in injury and disease. A probable factor in avascular necrosis. J. Bone Joint Surg. Am. 46, 509–516.
Strömqvist, B., 1983. Femoral head vitality after int racapsular hip fractures: 490 cases studied by intravital tetracycline labeling and Tc-MDP radionuclide imaging. Acta Orthop. Scand. 200, 1–71.
Strömqvist, B., Nilsson, L.T., Egund, N., Thorngren, K.G., Wingstrand, H., 1988. Intracapsular pressures in undisplaced fractures of the femoral neck. J. Bone Joint Surg. (Br.) 70, 192–194.
Sugamoto, K., Ochi, T., Takahashi, Y., Tamura, T., Matsuoka, T., 1998. Hemodynamic measurement in the femoral head using laser Doppler. Clin. Orthop. Relat. Res. 353, 138–147.
Swiontkowski, M., Tepic, P., Rahn, B., Perren, S., 1990. The effect of femoral neck fracture on femoral head blood flow. In: Bone circulation and bone necrosis, Fourth Symposium on Bone Circulation. Springer-Verlag, New York, pp. 150–153.
Wang, R., T., Y.S., 1985. He detection method and normal value of rabbit's abdominal aorta blood flow. J. Fourth Milit. Med. Univ. 6, 345–347.
Wentzel, J.J., Krams, R., Schuurbiers, J.C., 2001. Relationship between neointimal thickness and shear stress after Wallstent implantation in human coronary arteries. Circulation 103, 1740–1745.
Wu, Kai ea, 2000. The inner pressure of hip joint capsule and blood supply of femoral head. In: Thesis.
Yang, Y.M.L.Z., et al., 2004. The clinical application of nuclear radiography in femoral head fracture. Chin. J. Nucl. Med. Mol. Imaging 23, 205–206.
Zlotorowicz, M., Szczodry, M., Czubak, J., Ciszek, B., 2011. Anatomy of the medial femoral circumflex artery with respect to the vascularity of the femoral head. J. Bone Joint Surg. (Br.) 93, 1471–1474.